backgrounds was equal to half of the time required for the peak scan. The intensities of three standard reflections were measured every 1.5 h of X-ray exposure time for both compounds, and no decay with time was noted. The data were corrected for Lorentz, polarization, and background effects. The effects of absorption were not significant as judged by empirical ψ-scan data[11] (less than 3% in intensity), and therefore absorption corrections were not applied.

Solution and Refinement. The structures were solved by conventional heavy-atom techniques. The Ru atoms were located by Patterson syntheses. Full-matrix least-squares refinement and difference Fourier calculations were used to locate all remaining non-hydrogen atoms. The atomic scattering factors were taken from the usual tabulation,[12] and the effects of anomalous dispersion were included in F_c by using Cromer and Ibers'[13] values of $\Delta f'$ and $\Delta f''$. For compound **6** the positions of the phenyl and anion hydrogen atoms were calculated with use of the program HYDRO[1] (C–H distance set at 0.95 Å) and included in the structure factor calculations but were not refined. The Ru hydride in **6** was located by difference Fourier analysis. The positional parameters of the hydride were refined, but its thermal parameter was fixed. In compound **3**, the Ru hydrides were not located. The bridging SO_2CF_3 group was found to be disordered such that the S1, C3, and F3 atoms had two positions each with a 50% occupancy. The two positions, labeled primed and unprimed, were refined to give reasonable distances and angles. The two positions found for the bridging SO_2CF_3 correspond to isomers that result from tilting of the SCF_3 group in different directions. Only one of the two isomers is shown in Figure 2. Compound **3** was found to have a CH_2Cl_2 solvate molecule. As usual, this molecule was somewhat disordered and probably had partial occupancy. The distances and angles after refinement gave reasonable values. The final difference Fourier maps for both compounds did not reveal any significant residual electron density. The final positional and thermal parmeters of the refined atoms are given in Tables II and III and as supplementary material. Tables of observed and calculated structure factor amplitudes are inclined as supplementary material. ORTEP views of both compounds are shown in Figures 2 and 3 and as supplementary material.[5]

Acknowledgment. The authors are grateful to members of the 3M Analytical and Properties Research Laboratory for the spectroscopic and analytical data and to Robert Koshar, 3M Industrial and Consumer Sector Research Laboratory, for gifts of fluorocarbon acids. The 600-MHz ^{1}H NMR spectra were obtained at the Carnegie-Mellon University NMR Facility for Biomedical Studies. L.H.P. acknowledges support by the National Science Foundation for his contribution to this work.

Registry No. **1**, 428-76-2; **2**, 40906-82-9; **3**, 101011-69-2; **4**, 101141-60-0; **5**, 101011-70-5; **6**, 101011-71-6; **6a**, 101011-73-8; **8**, 101141-61-1; **9**, 101011-74-9; $(Ph_3P)_3RuH_2(CO)$, 25360-32-1; Ru, 7440-18-8.

Supplementary Material Available: Tables of distances and angles, general temperature factor expansions, least-squares planes, and observed and calculated structure factor amplitudes for **3** and **6**, a table of positional parameters for hydrogen atoms in **6**, ORTEP views of the $HC(SO_2CF_3)_2^-$ anions in **3** and **6**, and an ORTEP stereoview of the cation in **3** (66 pages). Ordering information is given on any current masthead page.

(12) Cromer, D. T.; Waber, J. T. "International Tables for X-Ray Crystallography"; Kynoch Press: Birmingham, England, 1974; Vol. IV, Table 2.2.4. Cromer, D. T. *Ibid*, Table 2.3.1.
(13) Cromer, D. T.; Ibers, J. A. In ref 12.

Contribution No. 7201 from the Arthur Amos Noyes Laboratory, California Institute of Technology, Pasadena, California 91125

Photophysics and Electrochemistry of Hexanuclear Tungsten Halide Clusters

Thomas C. Zietlow, Daniel G. Nocera, and Harry B. Gray*

Received May 30, 1985

The $W_6X_{14}^{2-}$ (X = Cl, Br, I) clusters possess emissive excited states characterized by microsecond lifetimes and large emission quantum yields (up to 0.39). The energy of the emissive state increases according to $W_6Cl_{14}^{2-}$ (1.83 eV) < $W_6Br_{14}^{2-}$ (1.85 eV) < $W_6I_{14}^{2-}$ (2.05 eV), which is the opposite trend from that expected when charge-transfer character is mixed into a primarily metal-localized transition. Variable-temperature emission data have been collected for the $(TBA)_2W_6X_8Y_6$ (Y = Cl, Br, I) clusters, indicating that the bridging halides (X) primarily determine the excited-state energy. The one-electron-oxidation potentials of the clusters also reflect the dominant electronic structural role of the bridging halides. The terminal halides (Y) have a substantial effect on the nonradiative decay rate, with k_{nr} decreasing according to Cl > Br > I.

Much of our work in inorganic photochemistry has centered on hexanuclear d^4 clusters, $M_6X_{14}^{2-}$ (M = Mo, W; X = Cl, Br, I), which feature long-lived excited states and several accessible oxidation levels.[1] On the basis of studies of the luminescences of $Mo_6Cl_{14}^{2-}$, $Mo_6Br_{14}^{2-}$, and $W_6Cl_{14}^{2-}$, we have suggested that the electronic transition that takes the emissive state to the ground state is primarily localized on the metal cluster core.[2] Further work has confirmed that a metal-localized description is correct for the $Mo_6X_{14}^{2-}$ series,[3] but the emissive behavior of the analogous tungsten clusters is more complicated.[4,5] In order to probe ligand effects on cluster properties more thoroughly, we have prepared the mixed halides $W_6X_8Y_6^{2-}$ (Y = Cl, Br, I) and have investigated their photophysical and electrochemical behavior.

Table I. Emission Data[a]

complex	λ_{max}, nm	τ, μs	ϕ_{em}	$10^{-4}k_r$, s^{-1}	$10^{-4}k_{nr}$, s^{-1}
$(TBA)_2W_6Cl_{14}$	833	1.5	0.02	1.3	65
$(TBA)_2W_6Cl_8Br_6$	814	2.3	0.04	1.7	42
$(TBA)_2W_6Cl_8I_6$	802	3.0	0.07	2.3	31
$(TBA)_2W_6Br_8Cl_6$	766	9.7	0.10	1.0	9.3
$(TBA)_2W_6Br_{14}$	758	15	0.15	1.0	5.7
$(TBA)_2W_6Br_8I_6$	752	15	0.25	1.7	5.0
$(TBA)_2W_6I_8Cl_6$	701	10	0.11	1.1	8.9
$(TBA)_2W_6I_8Br_6$	698	22	0.25	1.1	3.4
$(TBA)_2W_6I_{14}$	698	30	0.39	1.3	2.0

[a] Recorded in acetonitrile solution at 21 ± 2 °C; TBA = $(n\text{-}C_4H_9)_4N$.

Experimental Section

Cluster Compounds. $[(n\text{-}C_4H_9)_4N]_2Mo_6Cl_{14}$, $[(n\text{-}C_4H_9)_4N]_2Mo_6Br_{14}$, and $[(n\text{-}C_4H_9)_4N]_2W_6Cl_{14}$ were prepared as described previously.[2] The other $[(n\text{-}C_4H_9)_4N]_2W_6X_{14}$ clusters were obtained from alkali metal

(1) Maverick, A. W.; Gray, H. B. *J. Am. Chem. Soc.* **1981**, *103*, 1298.
(2) Maverick, A. W.; Najdzionek, J. S.; MacKenzie, D.; Nocera, D. G.; Gray, H. B. *J. Am. Chem. Soc.* **1983**, *105*, 1878.
(3) Zietlow, T. C.; Nocera, D. G.; Gray, H. B., unpublished observations.
(4) Zietlow, T. C.; Hopkins, M. D.; Gray, H. B. *J. Solid State Chem.* **1985**, *57*, 112.
(5) Zietlow, T. C.; Schaefer, W. P.; Sadeghi, B. S.; Hua, N.; Gray, H. B. *Inorg. Chem.*, in press.

0020-1669/86/1325-1351$01.50/0

Table II. Arrhenius Parameters[a]

complex	E_a, cm^{-1}	k_a, s^{-1}
$(TBA)_2W_6Cl_{14}$	2200	2.5×10^{10}
$(TBA)_2W_6Cl_8Br_6$	2200	2.1×10^{10}
$(TBA)_2W_6Cl_8I_6$	2300	1.8×10^{10}
$(TBA)_2W_6Br_8Cl_6$	2300	4.2×10^{9}
$(TBA)_2W_6Br_{14}$	2300	2.9×10^{9}
$(TBA)_2W_6Br_8I_6$	2400	2.4×10^{9}
$(TBA)_2W_6I_8Cl_6$	2100	1.2×10^{9}
$(TBA)_2W_6I_8Br_6$	2200	8.2×10^{8}
$(TBA)_2W_6I_{14}$	2200	8.2×10^{8}

[a] Data recorded in propylene carbonate solution; see Figure 1.

halide melt reactions.[6] The mixed halides $W_6X_8Y_6^{2-}$ were prepared according to the procedure of Hogue and McCarley.[7] Treatment of an aqueous HY solution of $W_6X_8Y_6^{2-}$ with $(n\text{-}C_4H_9)_4NY$ gave $[(n\text{-}C_4H_9)_4]_2W_6X_8Y_6$. All carbon, hydrogen, and nitrogen analyses were satisfactory.

Solvents. Acetonitrile and propylene carbonate were Burdick and Jackson reagent grade. The acetonitrile was dried over CaH_2 and then vacuum-transferred onto activated alumina. All solutions were degassed by repeated freeze–pump–thaw cycles.

Instrumentation. Absorption spectra were measured on a Cary 17 spectrophotometer. Emission spectra, which were recorded on an apparatus built at Caltech,[8] were corrected for monochromator and photomultiplier response. Emission lifetimes were obtained from least-squares fits to signal-averaged data on a PDP 11 computer interfaced to a Nd:YAG laser (fwhm = 8 ns; 355-nm excitation).

Electrochemical measurements were performed on PAR equipment (Model 175 universal programmer, Model 173 potentiostat, and Model 179 digital coulometer). Working and counter electrodes were platinum.

Results

The hexanuclear clusters $W_6X_8Y_6^{2-}$ are all luminescent in solution as well as in the solid. Data from the spectra[9] of all nine $W_6X_8Y_6^{2-}$ clusters in acetonitrile are given in Table I. In contrast to $Mo_6Cl_{14}^{2-}$, $Mo_6Br_{14}^{2-}$, and $Mo_6I_{14}^{2-}$, where the emissive excited state energies are virtually the same, the tungsten cluster emission spectra are halide-dependent. The energy of the emissive state increases in the $W_6X_{14}^{2-}$ spectra according to Cl (1.83 eV) < Br (1.85 eV) < I (2.05 eV).[10] This is the opposite trend from that expected when ligand-to-metal charge transfer character is mixed into a primarily metal-centered transition.

Emission lifetimes and quantum yields[11] were determined for the nine $W_6X_8Y_6^{2-}$ clusters in acetonitrile solution at 21 ± 2 °C (Table I). All emission decay traces displayed first-order kinetics over at least three lifetimes. The calculated radiative and nonradiative rates for the emissive excited states are given in Table I. The lifetime of the excited state increases in the order Y (terminal halide) = Cl < Br < I for a given bridging halide X. The quantum yield for emission follows the same trend, implying that the radiative rate for a particular cluster excited state is independent of the terminal halide.

Earlier experiments reported on these cluster systems established the temperature dependence of the lifetime of the excited state of crystalline $[(n\text{-}C_4H_9)_4N]_2M_6X_{14}$.[4] This work indicated that there is a nonradiative pathway that involves a level that is ≈2000 cm^{-1} above the emissive excited state in the tungsten clusters. In trying to understand the nature of this decay pathway, the temperature dependences of the lifetimes of all nine $[(n\text{-}C_4H_9)_4N]_2W_6X_8Y_6$ clusters were determined in propylene carbonate solution. Propylene carbonate was chosen because of its favorable solvent properties, its high boiling point (enabling a large temperature range to be examined in the experiment), and the similarity of the photophysics of the clusters in propylene carbonate and acetonitrile at room temperature. At relatively high temperatures, $k_{obsd} = k_a \exp(-E_a/kT)$ (Figure 1), and k_a varies with Y in the order I < Br < Cl for all the W_6X_8 cores (Table II). All of the cluster lifetimes are temperature-independent at low temperatures.

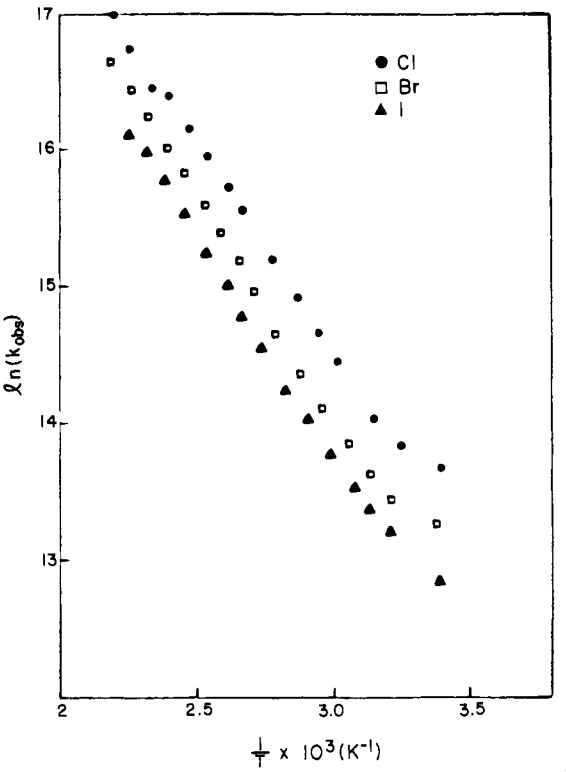

Figure 1. Arrenhius plot (ln k_{obsd} vs. $1/T$) for $(TBA)_2W_6Cl_8Y_6$ in propylene carbonate solution.

Table III. Oxidation Potentials[a]

complex	$E_{1/2}$(ox), V vs. SCE	complex	$E_{1/2}$(ox), V vs. SCE
$(TBA)_2W_6Cl_{14}$	1.12	$(TBA)_2W_6Br_{14}$	0.97
$(TBA)_2W_6Cl_8Br_6$	1.16	$(TBA)_2W_6I_{14}$	0.71
$(TBA)_2W_6Br_8Cl_6$	0.93		

[a] Data recorded in acetonitrile solution (0.1 M $(TBA)PF_6$) at 22 °C.

Cyclic voltammograms for the tungsten clusters were recorded. Not all of the oxidation couples are fully reversible, and with some of the clusters there is a problem with adsorption onto the platinum electrode. The half-wave potentials are given in Table III. For all the oxidation potentials listed as reversible, $i_{p,c} = i_{p,a}$, and a plot of $\nu^{1/2}$ vs. i_p is linear.[12] The reductive electrochemistry of the tungsten clusters does not appear to be reversible in any of the systems studied.

Discussion

It is apparent that the six terminal halides affect the emission energy only slightly, and this effect diminishes further as the inner core halides become larger. (The electronic interaction of the six tungsten atoms with the terminal halides is very small in the $W_6I_8^{4+}$ clusters.) This diminished interaction also may be inferred from the kinetic data, because the radiative rate of the $W_6I_8Y_6^{2-}$ excited state is independent of Y. These results correlate well with the structural data on the $W_6X_{14}^{2-}$ clusters, because the latter indicate that a bridging iodide is more strongly bound to the metal

(6) Sheldon, J. C. *J. Chem. Soc.* **1962**, 410.
(7) Hogue, R. D.; McCarley, R. E. *Inorg. Chem.* **1970**, *9*, 1355.
(8) Rice, S. F. Ph.D. Thesis, California Institute of Technology, 1982.
(9) Emission and absorption spectra are available as supplementary material.
(10) Emissive excited-state energies are estimated ν_{0-0} transitions from low-temperature emission spectra.
(11) Quantum yields were determined to ±20% by using $Ru(bpy)_3(PF_6)_2$ (ϕ_{em} = 0.062) in acetonitrile (Caspar, J. V.; Meyer, T. J. *J. Am. Chem. Soc.* **1983**, *105*, 5583).
(12) The peak separations were typically greater than 60 mV without compensation for solution resistance. There is further oxidative current as the potential is made more positive, but the couple is not at all reversible. Whether this denotes a structural change in the cluster [perhaps resulting in the formation of the M_6X_{18} structure with μ-halides (Kepert, D. L.; Marshall, R. E.; Taylor, D. J. *J. Chem. Soc., Dalton Trans.* **1974**, 506)] is being investigated.

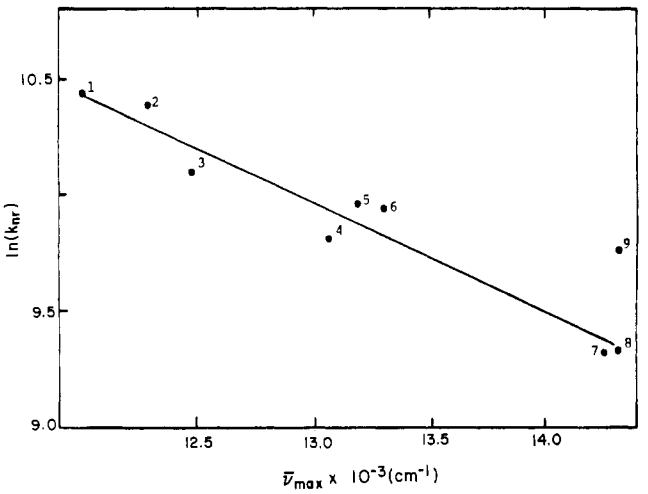

Figure 2. Plot of ln k_{nr} (77 K) vs. emission energy (corrected peak maxima). X, Y: (1) Cl, Cl; (2) Cl, Br; (3) Cl, I; (4) Br, Cl; (5) Br, Br; (6) Br, I; (7) I, Cl; (8) I, Br; (9) I, I.

cluster than a bridging chloride.[5] In all the tungsten clusters, however, the terminal halides markedly affect the nonradiative decay rates. The nonradiative pathway that is thermally activated in the temperature range 300–450 K is apparently not due to dissociation of a terminal halide, as large differences in the activation energies for the different halides would be expected. In fact, the differences are in the preexponential factor, with the iodide k_a being consistently smaller than the bromide, which is smaller still than the chloride.

The preexponential factors also seem to depend on the bridging halide, with a difference of about an order of magnitude between the clusters with bridging chlorides and those with bridging iodides. Since the activation energies are all about the same for this nonradiative pathway, this order of magnitude difference in k_a is responsible for the large difference in the room-temperature quantum yields and emission lifetimes of the various tungsten clusters with the same bridging halide. The fact that the largest k_a occurs for the smallest halide implies that the nonradiative pathway involves structural reorganization. The emission spectra of the clusters are consistent with a large distortion in the excited state,[13] and a structural deformation therefore may facilitate excited-state decay.

The rate of nonradiative decay of the excited state of each of the tungsten clusters levels off at low temperatures. The variation of ln k_{nr} (77 K) with emission energy (Figure 2) accords with the energy gap law;[14] the higher the energy of the emissive excited state, the lower the nonradiative decay rate of that state. Unfortunately, a detailed analysis of the type done on mononuclear systems[15] is not possible, owing to a lack of information on the important vibrational promoting and accepting modes in the clusters. However, the data do imply that the emissive states of all the tungsten clusters are similar; the increase in the emission energy upon exchange of halide is probably not due to different emissive states but rather to a greater splitting of the relevant molecular orbitals.

The redox potentials are also primarily a function of the metal and bridging halide. Comparison of the data in Table III with previous results[2] shows that any given tungsten cluster is more easily oxidized than its molybdenum analogue. What is more, the shift in oxidation potential upon exchange of bridging ligand corresponds to that expected on the basis of the electron-donor ability of the respective halide. The potentials are not affected substantially by the terminal ligands, confirming the conclusion reached from the emission data concerning the electronic structural dominance of the bridging halide.

Acknowledgment. We thank Mike Hopkins and Jay Winkler for helpful discussions. D.G.N. and T.C.Z. acknowledge graduate fellowships from the Sun Co. This work was supported by National Science Foundation Grant CHE84-19828.

Registry No. $W_6Cl_{14}^{2-}$, 47021-01-2; $W_6Br_{14}^{2-}$, 88477-00-3; $W_6I_{14}^{2-}$, 47021-02-3.

Supplementary Material Available: Figures of emission and absorption spectra of $(TBA)_2W_6X_8Y_6$ in acetonitrile solution (10 pages). Ordering information is given on any current masthead page.

(13) A distorted excited state is inferred from the observation that the emission bands are broad and structureless, even at low temperatures.
(14) Englman, R.; Jortner, J. *Mol. Phys.* **1970**, *18*, 145.
(15) Caspar, J. V.; Kober, E. M.; Sullivan, B. P.; Meyer, T. J. *J. Am. Chem. Soc.* **1982**, *104*, 630.